Journal of the European Ceramic Society 18 (1998) 1413–1418

PII: S0955-2219(98)00032-6
0955-2219/98/$—see front matter

Electrical Properties of New Type High Oxide Ionic Conductor $RE_{10}Si_6O_{27}$ (RE = La, Pr, Nd, Sm, Gd, Dy)

Susumu Nakayama[a]* and Masatomi Sakamoto[b]

[a]Department of Applied Chemistry and Biotechnology, Niihama National College of Technology, Niihama 792-8580, Japan

[b]Department of Material and Biological Chemistry, Faculty of Science, Yamagata University, Yamagatashi 990-8560, Japan

(Received 22 October 1997; revised version received 26 January 1998; accepted 2 February 1998)

Abstract

Electrical properties of the high oxide ionic conductive ceramic $RE_{10}Si_6O_{27}$ (RE = La, Pr, Nd, Sm, Gd, Dy) sintered at 1700–1800°C by the use of MgO-stabilized zirconia setter during a sintering have been investigated. The lowest activation energy and the highest conductivity at 200°C were achieved for $Pr_{10}Si_6O_{27}$ (55.4 kJ mol^{-1}) and $La_{10}Si_6O_{27}$ ($1{\cdot}32\times10^{-5}$ S cm^{-1}), respectively. The conductivity of $La_{10}Si_6O_{27}$ at 200°C was higher by order of $1{\cdot}5\times10^{1}$ times than that ($8{\cdot}82\times10^{-7}$ S cm^{-1} at 200°C) of $(Bi_2O_3)_{0.75}(Y_2O_3)_{0.25}$. The three-point bending strength of $La_{10}Si_6O_{27}$ was 100 MPa.

1 Introduction

The oxide ionic conductor is one of the most important ceramic electrolytes and has much potential for the application to sensors, fuel cells and oxygen pumps. Many oxide ionic conductors have been found and investigated actively over the last five decades. Among them, $(ZrO_2)_{0.92}(Y_2O_3)_{0.08}$, $(CeO_2)_{0.8}(GdO_{1.5})_{0.2}$ and $(Bi_2O_3)_{0.75}(Y_2O_3)_{0.25}$ having the fluorite-type structure and the perovskite type oxides, $La_{0.9}Sr_{0.1}Ga_{0.8}Mg_{0.2}O_3$ and $BaTh_{0.9}Gd_{0.1}O_3$, are well known to show the relatively high conductivities.[1–5] Recently, we reported that $RE_XSi_6O_{12+1.5X}$ (RE = La, Nd, Sm, Gd, Dy and X = 8–11) having a hexagonal apatite structure as the major phase shows oxide ionic conductivity.[6,7] Among these $RE_X(Si)_6O_{12+1.5X}$, $La_{10}Si_6O_{27}$ showed the highest conductivity. The conductivity at 300°C was $5{\cdot}54\times10^{-6}$ S cm^{-1} and this was almost equal to the conductivity ($3{\cdot}75\times10^{-6}$ S cm^{-1} at 300°C) of $(ZrO_2)_{0.92}(Y_2O_3)_{0.08}$. Here, the sintering temperature was 1550°C because $La_{10}Si_6O_{27}$ reacts with the alumina setter used for the support of $La_{10}Si_6O_{27}$ disc during a sintering above 1600°C. However, the sintering was not full at 1550°C. Fortunately, in this work we found that the MgO-stabilized zirconia does not react with $La_{10}Si_6O_{27}$ below 1800°C. This enabled us to raise the sintering temperature above 1600°C, resulting in the higher densification and the higher conductivity.

In this work, we present the electrical properties of the dense oxide ionic conductor $RE_{10}Si_6O_{27}$ (RE = La, Pr, Nd, Sm, Gd, Dy) sintered by the use of the MgO-stabilized zirconia setter instead of the alumina setter at 1700–1800°C.

2 Experimental

2.1 Samples

RE_2O_3 (99·9% - purity, Shin-etsu chemical Co., Ltd.) and SiO_2 (99·9% - purity, Kisan Metal Co., Ltd.) were used as the starting materials. The raw materials were mixed in ethanol with a ball-mill using Y_2O_3-stabilized zirconia ball (Daiichi Kigenso Kagaku Kogyo Co., Ltd.) and plastic pot, dried and then calcined in air at 1200°C for 2 h. The resultant powders were ball-milled into fine powders. After being dried, discs were prepared under a pressure of 100 MPa and sintered in air for 2 h. The sintered temperatures are given in Table 1. During the sintering process, discs were supported

*To whom correspondence should be addressed.

by a $(ZrO_2)_{0.915}(MgO)_{0.085}$ setter (Daiichi Kigenso Kagaku Kogyo Co., Ltd.).

The samples of $(ZrO_2)_{0.92}(Y_2O_3)_{0.08}$ and $(Bi_2O_3)_{0.75}(Y_2O_3)_{0.25}$ were pressed at 100 MPa and sintered for 2 h at 1650 and 1100°C, respectively, after the calcination of powder prepared by the conventional oxide mixing method. ZrO_2 (SPZ-grade), Bi_2O_3 (99·9%-purity) and Y_2O_3 (99·9%-purity) were purchased from Daiichi Kigenso Kagaku Kogyo Co., Ltd., Kisan Metal Co., Ltd. and Shin-etsu Chemical Co., Ltd., respectively.

2.2 Measurements

The microstructures and crystal structures were determined by scanning electron microscopy and powder X-ray diffraction, respectively. The prepared discs were 8 mm in diameter and 2 mm in thickness after sintering. After coating both sides of the disc with a Pt paste, it was baked at 950°C. The ac and dc electrical properties were measured using a multifrequency LCR meter (YHP 4192A) in the frequency range of 100 Hz to 10 MHz and an electrometer (Advantest TR8652), respectively. The sample was heated to 300°C in order to eliminate absorbed water prior to each measurement. The electromotive force, EMF, of the O_2 concentration cell, O_2+N_2, $Pt|La_{10}Si_6O_{27}|Pt$, Air($2{\cdot}1\times10^4$ Pa-O_2), was measured using an electrometer (Advantest TR8652) at each temperature in the O_2 partial pressure range of 10^3 to 10^5 Pa. The disc of $La_{10}Si_6O_{27}$ was sintered at 1700°C. After coating each side of the disc with a Pt paste, the disc was backed at 800°C. Then, Pt wires were connected. The disc was fixed on one-end of an alumina pipe with a glass cement. The reference electrode (air side) was inside. The O_2+N_2 and air were passed through the measuring and reference electrode at the flow rate of 100 $cm^3\,min^{-1}$, respectively. The three-point bending test was conducted according to the JIS R 1601 using the sintered samples ground to a size of 3×4×40 mm.

3 Results and Discussion

3.1 Microstructure and crystal structure

The densification was recognized above 1650°C and the highest density for each $RE_{10}Si_6O_{27}$ (RE = La, Pr, Nd, Sm, Gd, Dy) was obtained at the sintering temperature shown in Table 1. The fracture surface microstructures of $RE_{10}Si_6O_{27}$ (RE = La, Pr, Nd, Sm, Gd, Dy) are shown in Fig. 1. The densification is well progressed for all samples.

The major phases of all $RE_{10}Si_6O_{27}$ (RE = La, Pr, Nd, Sm, Gd, Dy) sintered at 1550–1850°C were the hexagonal apatite structure of composition, $RE_{9.33}\square_{0.67}(SiO_4)_6O_2$.[8] However, $RE_{10}Si_6O_{27}$ were not a single phase and the mixture of the apatite phase and a small amount of other crystal phases (RE_2SiO_5, etc.). The crystal structure (space group: $P6_3/m$) of the hexagonal apatite structure can be proposed as shown in Fig. 2. The a- and c-lattice constants estimated for each sample were constant regardless of the sintering temperature. The a- and c-lattice constants of $RE_{10}Si_6O_{27}$ (RE = La, Pr, Nd, Sm, Gd, Dy) increase monotonically with an increase in the ionic radius of RE, as can be seen from Fig. 3.

A hexagonal apatite structure phase was also confirmed as a major phase for $La_XSi_6O_{12+1.5X}$ (X = 8–11) and very weak peaks assignable to La_2SiO_5 were observed in their XRD patterns, indicating that these samples are not also a single phase. In $La_XSi_6O_{12+1.5X}$ (X = 8–11), the lattice constants were little changed by an increase in the X values.

3.2 Electrical properties

In order to determine the conductivity, complex plane impedance analysis was performed. The typical complex impedance plot obtained for $Sm_{10}Si_6O_{27}$, $Gd_{10}Si_6O_{27}$ and $Dy_{10}Si_6O_{27}$ gives two semicircles as shown in Fig. 4: one in the higher frequency region corresponds probably to the bulk component, whereas another in the lower frequency region corresponds to the grain boundary component. When the temperature increased, the size of the semicircle in the lower frequency decreased compared with that in the higher frequency. From these results, the conductivity (the sum of the bulk and grain boundary) was determined by extrapolation to zero reactance of the complex impedance plot. Figure 5 shows the typical complex impedance plot obtained for $La_{10}Si_6O_{27}$, $Pr_{10}Si_6O_{27}$ and $Nd_{10}Si_6O_{27}$. In the lower temperatures, the result was represented by a semicircle, probably corresponding to the bulk component, which passed through the origin in the high frequency region and had a spur, probably arising from the electrolyte-electrode behavior, in the low frequency region. The semicircle attributable to the grain boundary component is not observed, probably because the resistance of its component is fairly lower compared with that of bulk component. When the temperature was increased, the semicircle diminished and only a spur was observed. From these results, the conductivity was determined by the extrapolation to zero reactance of the complex impedance plot in the low frequency region. On the other hand, the complex impedance plots for $La_{10}Si_6O_{27}$, $Pr_{10}Si_6O_{27}$ and $Nd_{10}Si_6O_{27}$ sintered below 1600°C were similar to the typical complex impedance plot shown in Fig. 4.

Table 1. Sintering temperature and parameters of electrical properties

Material	*Sintering temperature* (°C)	*Activation energy* ($kJ\,mol^{-1}$)	*Conductivity* ($S\,cm^{-1}$)		
			300°C	*500°C*	*700°C*
$La_{10}Si_6O_{27}$	1700	62·2 (36·8)	$2{\cdot}42\times10^{-4}$	$4{\cdot}30\times10^{-3}$	$1{\cdot}08\times10^{-2}$
$Pr_{10}Si_6O_{27}$	1750	55·4 (30·4)	$9{\cdot}62\times10^{-5}$	$2{\cdot}83\times10^{-3}$	$6{\cdot}00\times10^{-3}$
$Nd_{10}Si_6O_{27}$	1750	59·1 (47·3)	$2{\cdot}10\times10^{-5}$	$3{\cdot}76\times10^{-4}$	$1{\cdot}89\times10^{-3}$
$Sm_{10}Si_6O_{27}$	1800	73·6 (69·1)	—	$4{\cdot}69\times10^{-5}$	$3{\cdot}90\times10^{-4}$
$Gd_{10}Si_6O_{27}$	1800	88·1	—	$1{\cdot}26\times10^{-6}$	$1{\cdot}71\times10^{-4}$
$Dy_{10}Si_6O_{27}$	1800	105·1	—	$7{\cdot}20\times10^{-8}$	$1{\cdot}86\times10^{-6}$

Parentheses denote the activation energy estimated in a higher temperature region.

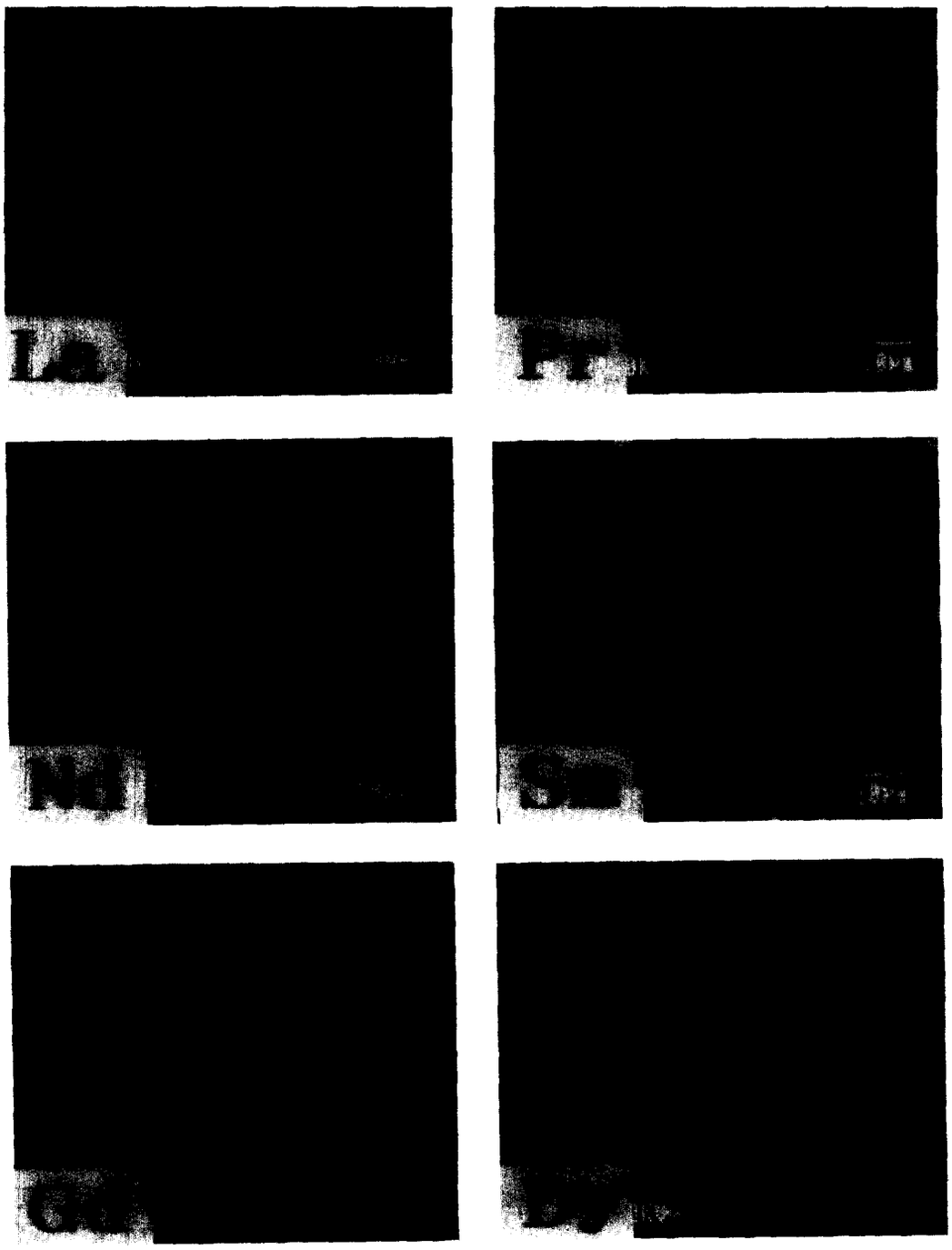

Fig. 1. Scanning electron micrographs of $RE_{10}Si_6O_{27}$ (RE = La, Pr, Nd, Sm, Gd, Dy).

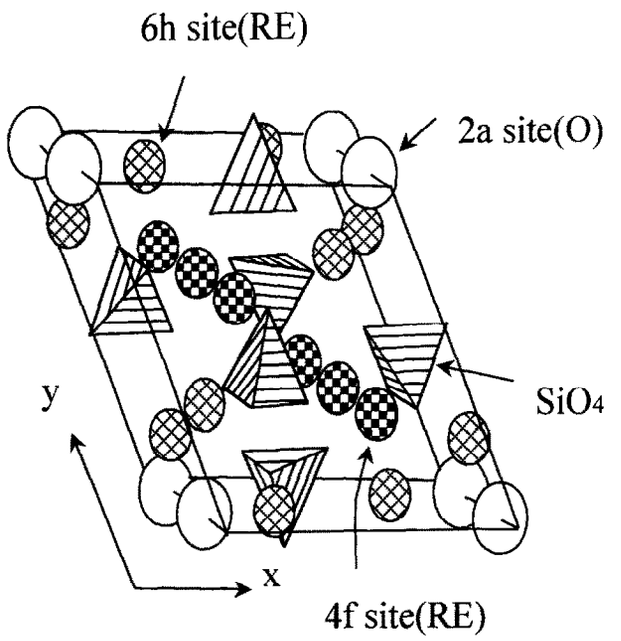

Fig. 2. Hexagonal apatite structure proposed to major phase of $RE_{10}Si_6O_{27}$ (RE = La, Pr, Nd, Sm, Gd, Dy).

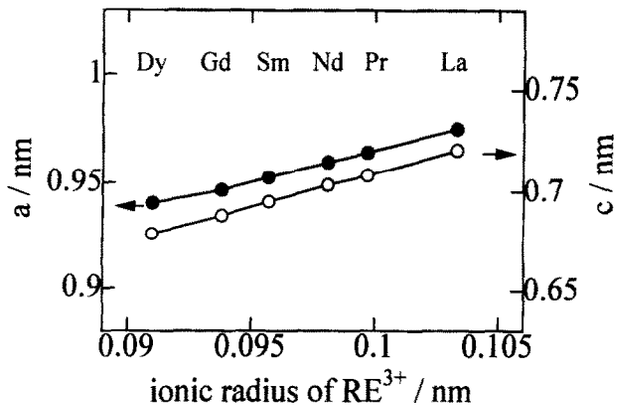

Fig. 3. Relationship between the ionic radius of RE^{3+} and the lattice constants of $RE_{10}Si_6O_{27}$ (RE = La, Pr, Nd, Sm, Gd, Dy).

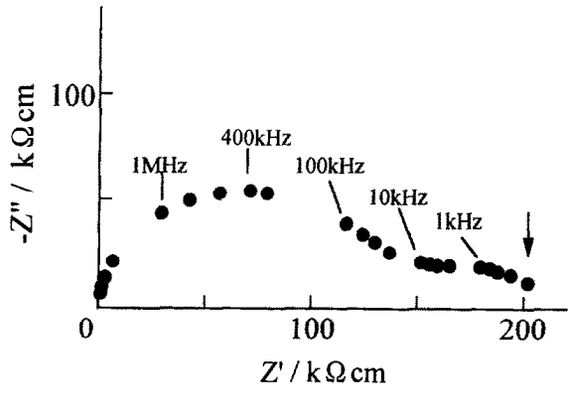

Fig. 4. Complex impedence plot of $Gd_{10}Si_6O_{27}$ at 600°C.

The conductivity data were parameterized by the Arrhenius equation.

$$GT = G_0 \exp(-E/kT)$$

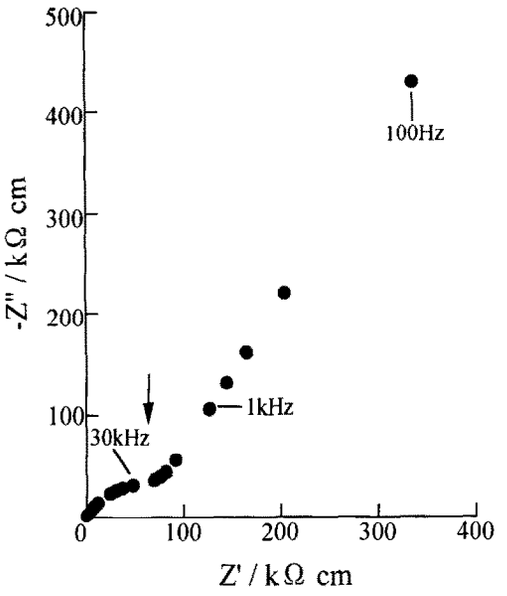

Fig. 5. Complex impedence plot of $La_{10}Si_6O_{27}$ at 200°C.

where G, G_0, E, k and T are the conductivity, pre-exponential factor, activation energy, Boltzmann constant and absolute temperature, respectively. Table 1 summarizes the electrical parameters of $RE_{10}Si_6O_{27}$ and the Arrhenius plots are shown in Fig. 6. The lowest activation energy and the highest conductivity at 200°C are achieved for $Pr_{10}Si_6O_{27}$ ($55{\cdot}4\,kJ\,mol^{-1}$) and $La_{10}Si_6O_{27}$ ($1{\cdot}32\times10^{-5}\,S\,cm^{-1}$), respectively. As can be seen in Fig. 7, the conductivity of $La_{10}Si_6O_{27}$ is higher than that of $(ZrO_2)_{0.92}(Y_2O_3)_{0.08}$ below 600°C and that of $(Bi_2O_3)_{0.75}(Y_2O_3)_{0.25}$ below 350°C. It is noteworthy that the conductivity ($1{\cdot}32\times10^{-5}$ $S\,cm^{-1}$) of $La_{10}Si_6O_{27}$ at 200°C is higher by order of $1{\cdot}5\times10^{1}$ times than that ($8{\cdot}82\times10^{-7}\,S\,cm^{-1}$) of

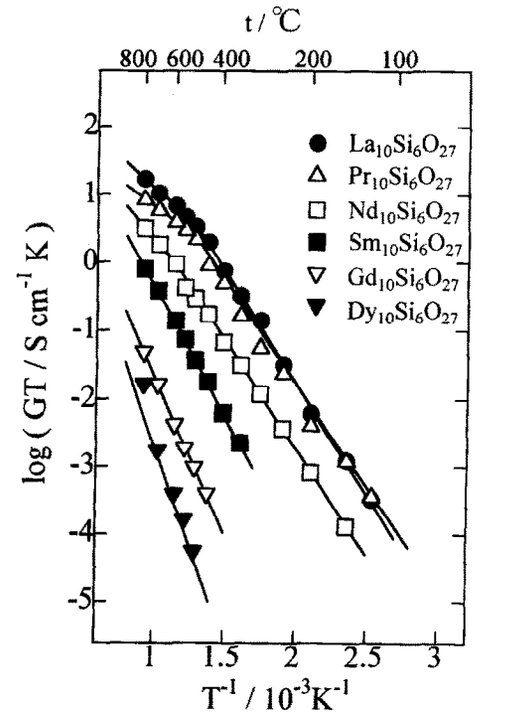

Fig. 6. Temperature dependence of conductivity.

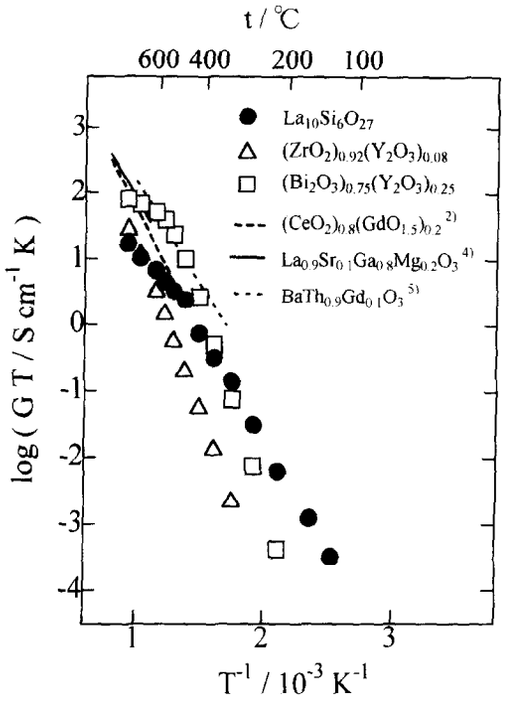

Fig. 7. Temperature dependence of conductivity.

$(Bi_2O_3)_{0.75}(Y_2O_3)_{0.25}$ which is known to show the high conductivity at low temperature thus far. On the other hand, the conductivity of $La_{10}Si_6O_{27}$ is lower than the typical conductivities of $(CeO_2)_{0.8}(GdO_{1.5})_{0.2}$, $La_{0.9}Sr_{0.1}Ga_{0.8}Mg_{0.2}O_3$ and $BaTh_{0.9}Gd_{0.1}O_3$, in the higher temperature.[2,4,5] The appearance of inflection point in the slope of Arrhenius plots for $RE_{10}Si_6O_{27}$ (RE = La, Pr, Nd, Sm) was concluded not to be attributable to a phase transformation from the results of the high temperature powder X-ray diffraction pattern in the room temperature to 1200°C. Furthermore, the conductivities of $RE_{10}Si_6O_{27}$ did not change for 3 months in air.

Figure 8 shows the relationship between the ionic radius of RE^{3+} and the electrical properties of $RE_{10}Si_6O_{27}$ (RE = La, Pr, Nd, Sm, Gd and Dy). The conductivity at 500°C increases with an increase in the ionic radius of RE^{3+} for $RE_{10}Si_6O_{27}$. On the other hand, the activation energy increases with increasing ionic radius of RE^{3+} from Pr to La and decreasing radius from Pr to Dy.

As shown in Fig. 9, the highest conductivity and the lowest activation energy in $La_XSi_6O_{12+1.5X}$ (X = 8–11) were observed for X = 10, where the X-values is a little larger than X = 9.33 for the composition of apatite structure, $La_{9.33}\square_{0.67}(SiO_4)_6O_2$.

3.3 EMF of oxygen concentration cell with $La_{10}Si_6O_{27}$ electrolyte

The O_2 gas concentration cell was used to confirm the ionic conduction of $La_{10}Si_6O_{27}$ sintered at 1700°C. The EMF between the two electrodes obeys the Nernst equation,

$$EMF = (RT/nF)\ln(P_{O2}/P'_{O2})$$

where R, T, n, F, P_{O2} and P'_{O2} are the gas constant, absolute temperature, electron transfer number, Faraday constant, O_2 partial pressure at the measuring electrode, and O_2 partial pressure at the reference electrode ($P'_{O2} = 2{\cdot}1 \times 10^4$ Pa), respectively. Table 2 summarizes the theoretical and experimental Nernstian slopes and electron transfer numbers for the O_2 gas concentration cell at each temperature. The observed EMF was in good agreement with the theoretical value and the n values were close to 4, indicating that this response

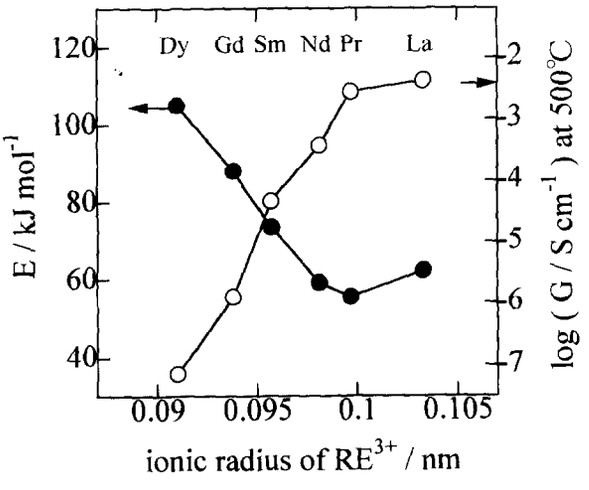

Fig. 8. Relationship between the ionic radius of RE^{3+} and the electrical properties of $RE_{10}Si_6O_{27}$ (RE = La, Pr, Nd, Sm, Gd, Dy).

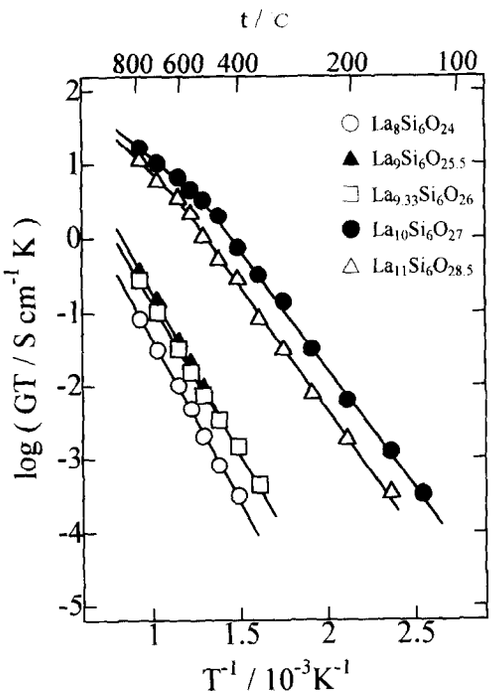

Fig. 9. Temperature dependence of conductivity.

Table 2. Theoretical and experimental Nernstian slopes and electron transfer number (n) for O_2 gas concentration cell using $La_{10}Si_6O_{27}$ as the solid electrolyte

Temperature (°C)	*Slpoe* (*mV decade*$^{-1}$)		
	Theoretical ($n=4$)	*Observed*	n
450	36·82	22·0	6·5
500	38·30	35·6	4·3
600	43·26	42·1	4·1
700	48·21	44·0	4·4

must be caused by the four-electron reaction of O_2 molecules at the electrodes above 500°C. The current responses for a potential change from +1 to −1 V of Pt|$La_{10}Si_6O_{27}$|Pt were measured in an N_2 atmosphere. A current flowed momentarily after the polar changes and then gradually approached zero. Furthermore, the conductivity determined by the dc method was considerably lower than that determined by the ac method. These results show that the major charge carriers are not electron and not also hole but ion, though the kind of ion is not unclear at present.

3.4 Mechanical property of $La_{10}Si_6O_{27}$

The three-point bending strength of $La_{10}Si_6O_{27}$ sintered at 1700°C was 100 MPa. This strength is 2 times higher than that (50 MPa) of $(Bi_2O_3)_{0.75}(Y_2O_3)_{0.25}$ and equal to that of the reaction-bonded silicon nitride which is known as the engineering ceramics, whereas it is lower than that (200 MPa) of $(ZrO_2)_{0.92}(Y_2O_3)_{0.08}$.

4 Conclusions

New type high oxide ionic conductors $RE_{10}Si_6O_{27}$ (RE = La, Pr, Nd, Sm, Gd, Dy) were synthesized by the use of MgO-stabilized zirconia setter during a sintering. Their microstructures, crystal structures and electrical properties and the experimental electromotive force of oxygen concentration cell with $La_{10}Si_6O_{27}$ were examined. The results are summarized as follows:

1. The densification was well progressed for $RE_{10}Si_6O_{27}$ (RE = La, Pr, Nd, Sm, Gd, Dy) sintered at 1700–1800°C. The major phases of all samples were the hexagonal apatite structure. The a- and c-lattice constants of $RE_{10}Si_6O_{27}$ increased monotonically with an increase in the ionic radius of RE^{3+}.
2. The lowest activation energy and the highest conductivity at 200°C were achieved for $Pr_{10}Si_6O_{27}$ (55·4 kJ mol^{-1}) and $La_{10}Si_6O_{27}$ ($1{\cdot}32\times10^{-5}$ S cm^{-1}), respectively. The conductivity of $La_{10}Si_6O_{27}$ was higher than that of $(ZrO_2)_{0.92}(Y_2O_3)_{0.08}$ below 600°C and that of $(Bi_2O_3)_{0.75}(Y_2O_3)_{0.25}$ below 350°C. The conductivity of $La_{10}Si_6O_{27}$ at 200°C was higher by order of $1{\cdot}5\times10^{1}$ times than that ($8{\cdot}82\times10^{-7}$ S cm^{-1} at 200°C) of $(Bi_2O_3)_{0.75}(Y_2O_3)_{0.25}$. The activation energy of $RE_{10}Si_6O_{27}$ (RE = La, Pr, Nd, Sm, Gd, Dy) was increased with increasing ionic radius of RE^{3+} from Pr to La and decreasing radius from Pr to Dy.
3. The EMF in the O_2 gas concentration cell comprising $La_{10}Si_6O_{27}$ agreed with the theoretical electromotive force calculated from the Nernst equation above 500°C, suggesting that the response is due to the four-electron reaction of O_2 molecules at the electrodes. The conductivity determined by the dc method was considerably lower than that determined by the ac method.
4. The three-point bending strength of $La_{10}Si_6O_{27}$ was 100 MPa.

Acknowledgements

The authors thank Mr S. Kakita, Mr Y. Masuda, Mr T. Suzuki and Mr K. Itoh of Daiichi Kigenso Kagaku Kogyo Co., Ltd. for their cooperation and Mr R. Yajima, a former managing director of Shinagawa Refractories Co., Ltd., for his helpful advice.

References

1. Takahashi, T., *High Conductivity Solid Ionic Conductors*. World Scientific, Singapore, 1987, pp 402–446.
2. Kudo, T. and Obayashi, H., Mixed electrical conduction in the fluorite-type $Ce_{1-x}Gd_xO_{2-x/2}$. *J. Electrochem. Soc.*, 1976, **123**, 415–419.
3. Takahashi, T., Iwahara, H. and Arao, T., High oxide ion conduction in sintered oxides of the system Bi_2O_3–Y_2O_3. *J. Appl. Electrochem.*, 1975, **5**, 187–195.
4. Ishihara, T., Matsuda, H. and Takita, Y., Doped $LaGaO_3$ perovskite type oxide as a new oxide ionic conductor. *J. Am. Chem. Soc.*, 1994, **116**, 3801–3803.
5. Cook, R. L., Osborne, J. J., White, J. H., MacDuff, R. C. and Sammells, A. F., Investigations on $BaTh_{0.9}Gd_{0.1}O_3$ as an intermediate temperature fuel cell solid electrolyte. *J. Electrochem. Soc.*, 1992, **139**, L19-20.
6. Nakayama, S., Aono, H. and Sadaoka, Y., Ionic conductivity of $Ln_{10}(SiO_4)_6O_3$ (Ln = La,Nd,Sm,Gd and Dy). *Chem.Lett.*, 1995, 431–442.
7. Nakayama, S., Kageyama, T., Aono, H. and Sadaoka, Y., Ionic conductivity of lanthanoid silicates, $Ln_{10}(SiO_4)_6O_3$ (Ln = La, Nd, Sm, Gd, Dy, Y, Ho, Er and Yb). *J. Mater. Chem.*, 1995, **5**, 1801—1805.
8. Felsche, J., Rare earth silicates with the apatite structure. *J. Solid State Chem.*, 1972, **5**, 266–275.